This article was downloaded by: [University of Missouri Columbia]
On: 31 August 2012, At: 11:54
Publisher: Taylor & Francis
Informa Ltd Registered in England and Wales Registered Number: 1072954 Registered office: Mortimer House, 37-41 Mortimer Street, London W1T 3JH, UK

Transactions of the American Fisheries Society
Publication details, including instructions for authors and subscription information:
http://www.tandfonline.com/loi/utaf20

A Remote-Sensing, GIS-Based Approach to Identify, Characterize, and Model Spawning Habitat for Fall-Run Chum Salmon in a Sub-Arctic, Glacially Fed River

Lisa Wirth [a], Amanda Rosenberger [b], Anupma Prakash [c], Rudiger Gens [c], F. Joseph Margraf [a e] & Toshihide Hamazaki [d]

[a] U.S. Geological Survey, Alaska Cooperative Fish and Wildlife Research Unit, Post Office Box 757020, Fairbanks, Alaska, 99775-7020, USA

[b] School of Fisheries and Ocean Sciences, University of Alaska Fairbanks, Post Office Box 757220, Fairbanks, Alaska, 99775, USA

[c] Geophysical Institute, University of Alaska Fairbanks, Post Office Box 7320, Fairbanks, Alaska, 99775, USA

[d] Alaska Department of Fish and Game, Division of Commercial Fisheries, 333 Raspberry Road, Anchorage, Alaska, 99518, USA

[e] U.S. Geological Survey, Box 25046 MS 406 DFC, Denver, Colorado, 80225, USA

Version of record first published: 30 Aug 2012

To cite this article: Lisa Wirth, Amanda Rosenberger, Anupma Prakash, Rudiger Gens, F. Joseph Margraf & Toshihide Hamazaki (2012): A Remote-Sensing, GIS-Based Approach to Identify, Characterize, and Model Spawning Habitat for Fall-Run Chum Salmon in a Sub-Arctic, Glacially Fed River, Transactions of the American Fisheries Society, 141:5, 1349-1363

To link to this article: http://dx.doi.org/10.1080/00028487.2012.692348

PLEASE SCROLL DOWN FOR ARTICLE

Full terms and conditions of use: http://www.tandfonline.com/page/terms-and-conditions

This article may be used for research, teaching, and private study purposes. Any substantial or systematic reproduction, redistribution, reselling, loan, sub-licensing, systematic supply, or distribution in any form to anyone is expressly forbidden.

The publisher does not give any warranty express or implied or make any representation that the contents will be complete or accurate or up to date. The accuracy of any instructions, formulae, and drug doses should be independently verified with primary sources. The publisher shall not be liable for any loss, actions, claims, proceedings, demand, or costs or damages whatsoever or howsoever caused arising directly or indirectly in connection with or arising out of the use of this material.

Transactions of the American Fisheries Society 141:1349–1363, 2012
© American Fisheries Society 2012
ISSN: 0002-8487 print / 1548-8659 online
DOI: 10.1080/00028487.2012.692348

ARTICLE

A Remote-Sensing, GIS-Based Approach to Identify, Characterize, and Model Spawning Habitat for Fall-Run Chum Salmon in a Sub-Arctic, Glacially Fed River

Lisa Wirth*
U.S. Geological Survey, Alaska Cooperative Fish and Wildlife Research Unit, Post Office Box 757020, Fairbanks, Alaska 99775-7020, USA

Amanda Rosenberger
School of Fisheries and Ocean Sciences, University of Alaska Fairbanks, Post Office Box 757220, Fairbanks, Alaska, 99775, USA

Anupma Prakash and Rudiger Gens
Geophysical Institute, University of Alaska Fairbanks, Post Office Box 7320, Fairbanks, Alaska, 99775, USA

F. Joseph Margraf[1]
U.S. Geological Survey, Alaska Cooperative Fish and Wildlife Research Unit, Post Office Box 757020, Fairbanks, Alaska 99775-7020, USA

Toshihide Hamazaki
Alaska Department of Fish and Game, Division of Commercial Fisheries, 333 Raspberry Road, Anchorage, Alaska, 99518, USA

Downloaded by [University of Missouri Columbia] at 11:54 31 August 2012

Abstract

At northern limits of a species' distribution, fish habitat requirements are often linked to thermal preferences, and the presence of overwintering habitat. However, logistical challenges and hydrologic processes typical of glacial systems could compromize the identification of these habitats, particularly in large river environments. Our goal was to identify and characterize spawning habitat for fall-run chum salmon *Oncorhynchus keta* and model habitat selection from spatial distributions of tagged individuals in the Tanana River, Alaska using an approach that combined ground surveys with remote sensing. Models included braiding, sinuosity, ice-free water surface area (indicating groundwater influence), and persistent ice-free water (i.e., consistent presence of ice-free water for a 12-year period according to satellite imagery). Candidate models containing persistent ice-free water were selected as most likely, highlighting the utility of remote sensing for monitoring and identifying salmon habitat in remote areas. A combination of ground and remote surveys revealed spatial and temporal thermal characteristics of these habitats that could have strong biological implications. Persistent ice-free sites identified using synthetic aperture radar appear to serve as core areas for spawning fall chum salmon, and the importance of stability through time suggests a legacy of successful reproductive effort for this homing species. These features would not be captured with a one-visit traditional survey but rather required remote-sensing monitoring of the sites through time.

*Corresponding author: lmwirth@alaska.edu
[1]Present address: U.S. Geological Survey, Box 25046 MS 406 DFC, Denver, Colorado 80225, USA.
Received January 31, 2012; accepted May 2, 2012

Downloaded by [University of Missouri Columbia] at 11:54 31 August 2012

Conducting a habitat study of a species at the extremes of their range can simplify identification of limiting factors; a single environmental condition could be constraining range expansion of the species (Stearns 1977). For example, at northern limits of a species' range, the fundamental habitat requirement and limiting factor may be as simple as liquid water due to severe winter conditions (e.g., freezing, frazil ice, or subzero temperatures). However, this simplification can be compromised by variability in that limiting factor; small changes in environmental conditions could have dramatic consequences. Changing weather conditions from year-to-year, for example, could result in high temporal variability in the presence of liquid water for overwintering fish. Incorporation of long-term data, however, could allow researchers to understand what is 'average' for a particular location and permit detection of long-term trends.

Pacific salmon are anadromous, returning to their natal site to spawn, honing in on hydrological features such as water odor, depth, and velocity, gravel composition, and the presence of cover (Salo 1991). The homing nature of salmon is such that their present distribution and habitat use not only reflect the suitability of habitat at the time of observation, but also the suitability of those areas in years past. The presence of suitable temperatures for egg incubation and juvenile rearing is probably very important, particularly in the northern limits of their range in Alaska. However, the dynamic nature of the Arctic and sub-Arctic environments of Alaska (Milner et al. 1995) highlights the importance of understanding temporal variation in physical processes determining the distribution of salmon species. It is unfortunate, then, that long-term data sets for this region are generally unavailable.

The Yukon River drainage in Alaska possesses two genetically distinct life history forms of chum salmon *Oncorhynchus keta*, summer and fall runs (Seeb and Crane 1999). This species matures and returns to the freshwater environment between ages 3 and 6, and fry emerge and migrate to the ocean in spring during ice-out (Quinn 2005). Fall-run chum salmon begin their spawning migration and enter the Yukon River from late June through early September and spawn in main-stem habitats (Barton 1992). Peak spawning is from mid-October to mid-November, coinciding with decreasing, silty glacial run-off (silt can be detrimental to the survival of salmon eggs; Hausle and Coble 1976; Lapointe et al. 2004; Levasseur et al. 2006) and increased water clarity (Osterkamp 1975). However, late spawning leads to a narrow time window for egg incubation and larval growth prior to spring smolt outmigration. In the northernmost (Arctic and sub-Arctic) regions, areas of upwelling water may offset this disadvantage. Areas with upwelling groundwater or hyporheic exchange provide warmer and more consistent water temperatures for winter incubation and protection from freezing (Reynolds 1997; Fausch et al. 2002; Quinn 2005). A number of studies in other parts of their range have documented the selection of upwelling water for spawning salmon (Reynolds 1997; Geist and Dauble 1998; Baxter and Hauer 2000; Geist et al. 2002).

The goal of our study was to identify and characterize spawning habitat for fall chum salmon and model habitat selection in the main-stem Tanana River, a tributary of the Yukon River at the northern extent of the chum salmon's range, where subzero temperatures and winter conditions are extended and severe. We characterized habitat along an extensive reach of the Tanana River, with particular note of areas of ice-free water during winter, which indicated the presence of groundwater. Given the importance of a legacy of spawning success for this homing species, we also characterized the temporal consistency of these ice-free areas using remotely sensed data collected over the last decade. Finally, to determine the relative importance of groundwater influence on spawning-female reach selection, we related numbers of spawning females to reach characteristics, including the presence of ice-free areas (indicating strong groundwater influence), the permanence of those areas (consistent presence from year to year), and other habitat features that may also play a role in spawning-female habitat selection. Given the potential importance of groundwater-influenced areas (i.e., ice-free) for spawning chum salmon, we collected data to characterize both spatial (through remote-sensing techniques) and temporal (through on-site temperature loggers) thermal characteristics of ice-free areas that persisted over our period of investigation. We anticipated that this approach would demonstrate potential for integrating remote sensing technologies and in-stream data collection for future studies to better elucidate critical habitat characteristics for a commercially and culturally important fish species.

METHODS

Study area.—This study took place in the Tanana River, a large, free-flowing, glacially fed tributary of the Yukon River (Figure 1). This is the largest tributary of the Yukon River, flowing 700 km northwest through a broad alluvial valley, draining an area of 155,250 km^2. Heavily silted and braided, the Tanana River poses challenges for monitoring and identifying spawning fish and spawning areas. Turbid waters interfere with visual identification of spawning congregations, and the habitat complexity of a large but braided channel can also complicate standard riverine habitat assessments designed for small to medium streams (e.g., Thomson et al. 2001). Runs of fall chum salmon return to the Tanana River and support important subsistence, personal use, and commercial fisheries. However, in recent years, fall chum salmon runs returning to the Yukon River and, consequently, the Tanana River, have been in decline (Borba et al. 2009).

Prior to our study, the only rivers regularly monitored for chum salmon escapements (after the subsidence of glacial waters) were the Toklat (average escapement, 31,000) and Delta (14,000) rivers, tributaries to the Tanana River (Bue et al. 2004). Prior to this study, it was unknown but suspected that chum salmon spawned in the main-stem river, which is the focus of our study. Our study area, located between Fairbanks and Big

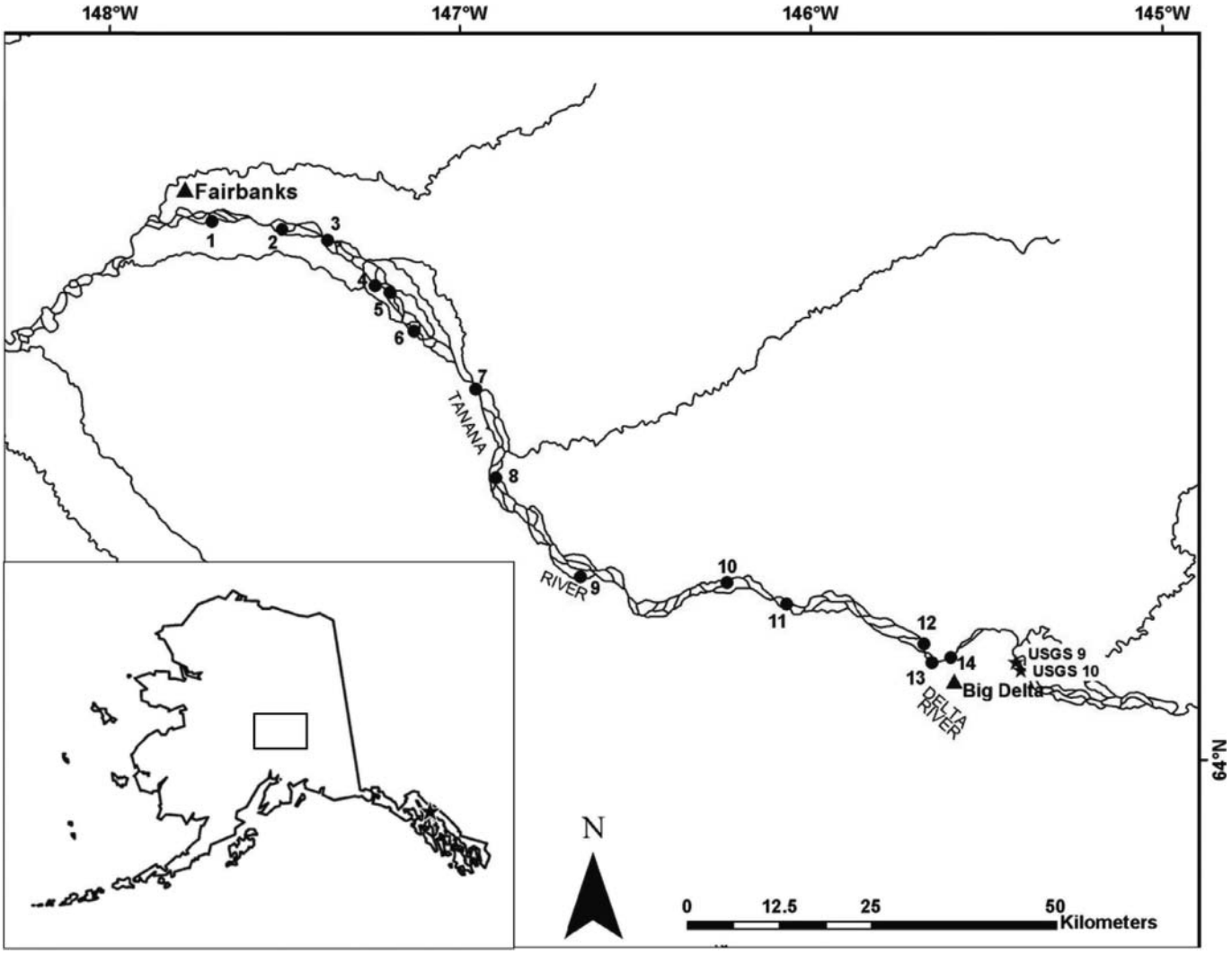

FIGURE 1. Main-stem Tanana River study area between Fairbanks and Big Delta, Alaska. Numbers indicate locations of retrieved surface temperature data loggers.

Downloaded by [University of Missouri Columbia] at 11:54 31 August 2012

Delta, Alaska (Figure 1), was 160 river kilometers in length and subdivided into 16 study reaches, each approximately 10 km long (reach length range: 9.4–12.1 km; Table 1). In establishing reaches we took into account smaller tributaries that empty into the Tanana River such that a tributary did not enter in the middle of a reach; this lead to variability in reach length.

Radiotelemetry data.—Adult female fall chum salmon ($N = 328$) were captured with fish wheels upstream of the Kantishna River on the north bank of the Tanana River from 16 August through 30 September 2008 (Yukon River mile 793), between the communities of Manley and Old Minto. Fish were tagged with an internal pulse-coded radio transmitter manufactured by Advanced Telemetry Systems, Inc. (ATS 2008). Transmitters weighed approximately 20 g, were 5.4 cm long and 2.0 cm in diameter, and had a 30-cm transmitting antenna. Surveys to track fish movement were conducted by air at least twice weekly beginning 2 weeks after initial tag deployment until late December.

Satellite imagery.—Multiple, complementary imagery data sets were used to provide the most accurate and extensive imagery (both in space and through time) possible for the study site and to verify findings and methodology. The RADARSAT-1 images acquired by the Alaska Satellite Facility (ASF) were used to determine persistence of ice-free water. Synthetic aperture radar (SAR) satellites, like RADARSAT-1, image by transmitting electromagnetic signals towards the earth's surface and then receiving the portion of electromagnetic signal that is backscattered towards the satellite. The signal has the capability to penetrate cloud cover, allowing for data collection irrespective of weather (Cumming and Wong 2005), a useful feature for the Alaska environment. The images were collected from the C-band (5.7-cm wavelength) and were taken from the fine beam

TABLE 1. Habitat characteristics and lengths of the 16 study reaches in the Tanana River, Alaska. All habitat variables were used in candidate models of the total number of spawners in the Tanana River.

Reach number	Length (km)	Sinuosity	Braiding	Ice-free surface area (km^2)	Persistent ice-free water	Total number of spawners
1	9.4	1.36	2.19	1.09	1	22
2	10.5	1.20	2.18	0.27	1	14
3	12.1	1.19	2.88	0.57	1	41
4	12.1	1.29	3.49	0.08	0	8
5	10.1	1.32	3.24	0.07	0	5
6	10.3	1.23	2.95	0.01	0	3
7	9.7	1.14	3.01	0.15	1	21
8	9.5	1.28	2.93	0.06	0	14
9	9.6	1.46	3.58	0.00	0	16
10	9.5	1.36	3.84	0.05	0	17
11	9.6	1.30	4.30	0.06	0	14
12	10.3	1.32	3.69	0.13	0	10
13	10	1.19	4.28	0.20	0	5
14	9.8	1.19	4.26	0.14	0	4
15	10	1.14	3.02	0.04	0	1
16	9.8	1.22	2.50	0.02	0	2

Downloaded by [University of Missouri Columbia] at 11:54 31 August 2012

and standard beam mode. Fine beam has a spatial resolution of 6.25 m; while the standard beam has a spatial resolution of 12.5 m. Fine-beam images were ideal due to their higher spatial resolution but did not give complete coverage of the study area, resulting in the need to use standard-beam images for the southern reaches. Fine-beam data were collected in March 1996, February 2005, and March 2008, corresponding to late winter when discharge in the river is groundwater-based. Standard-beam images from 1997, 2005, and 2008 were initially examined in conjunction with the fine-beam images to create complete coverage for the study area. A preliminary analysis of ice-free areas for these 3 years identified spatially persistent ice-free areas. To further confirm their persistence through time, additional years of imagery were analyzed (standard beam images for March 1997, 2000–2003, 2005, 2006, and 2008). Yearly observations during the time frame were not available, and these years were selected because they contained the most complete coverage of the study area during late winter (March; Table 2).

Interpretation of SAR images is not immediately intuitive due to the side-looking SAR geometry and the complex interaction of the SAR signal with the target. The intensity of a SAR pixel represents the amount of signal backscattered from the target area (Gens 2009). Among several factors that control the backscatter, two important factors are the amount of moisture (that, in turn, controls the dielectric property) and surface texture of the target (Pietroniro et al. 2005). Dielectric properties for liquid water are different from snow and ice, which can vary greatly depending on the amount of liquid water contained in the snow or ice particles (Fung and Ulaby 1983; Simonett and Davis 1983). The presence of still or slowly flowing water (without surface turbulence) enhances contrast in the radar signal because it acts as a specular reflector with a low backscatter signal (Pietroniro et al. 2005). Ice-free areas of liquid water surrounded by snow and ice appeared dark, whereas the surrounding snow and ice provided a bright signal on the image. The effect of surface roughness of the ice-free areas in the radar return was negligible.

Images from the advanced visible and near infrared radiometer type 2 (AVNIR-2) onboard the advanced land observation satellite (ALOS) were used as base imagery to identify final spawning location and to calculate the ice-free water surface area

TABLE 2. Synthetic aperture radar (SAR) images used to identify ice-free areas in the Tanana River.

Granule identifcation	Beam mode	Acquisition date
R1_01952_FN1_F162	Fine beam	Mar 20, 1996
R1_01952_FN1_F161	Fine beam	Mar 20, 1996
R1_06897_ST6_F160	Standard beam 6	Mar 01, 1997
R1_22675_ST6_F160	Standard beam 6	Mar 09, 2000
R1_27877_ST3_F161	Standard beam 3	Mar 08, 2001
R1_33022_ST3_F161	Standard beam 3	Mar 03, 2002
R1_38224_ST1_F161	Standard beam 1	Mar 02, 2003
R1_48600_FN1_F162	Fine beam	Feb 25, 2005
R1_48600_FN1_F161	Fine beam	Mar 25, 2005
R1_48722_ST1_F290	Standard beam 1	Mar 05, 2005
R1_53981_ST7_F290	Standard beam 7	Mar 08, 2006
R1_64435_ST2_F160	Standard beam 2	Mar 09, 2008
R1_64457_FN1_F289	Fine beam	Mar 10, 2008
R1_64457_FN1_F288	Fine beam	Mar 10, 2008

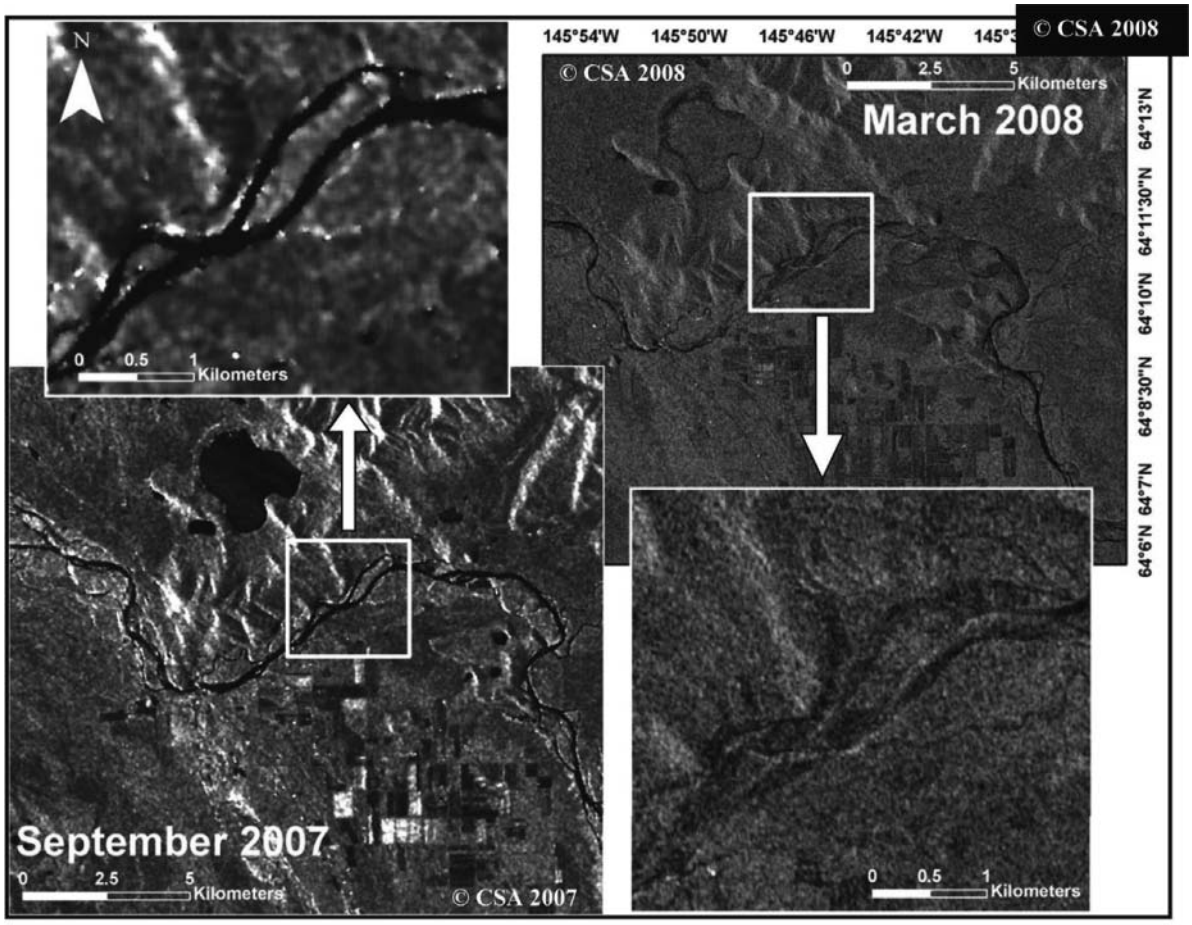

FIGURE 2. Image of the Tanana River illustrating an easily identifiable water signature in September prior to river freeze-up. The frozen river in late winter (March) is less obvious, blending with the surrounding area due to similar radar signatures.

in 2009. The AVNIR-2 sensor acquires four bandwidths, three visible bands (0.42–0.50 μm, 0.52–0.60 μm, 0.61–0.69 μm) and one near-infrared band (0.76–0.89 μm) with 10-m spatial resolutions. The images were acquired in March 2009, and all had 30% or less cloud cover.

Total river surface area, prior to river freeze-up, was calculated by manually digitizing the limits of the water body in ArcGIS (ESRI 2007) on the SAR images acquired from the standard beam mode via a 12.5-m spatial resolution collected on September 30, 2007 (Figure 2). The same SAR images were used to calculate river-braiding index and sinuosity, described below. The AVNIR-2 images of March 2009 (after river freeze-up and during base flow winter conditions; U.S. Geological Survey [USGS] Water Resources Data, Nenana, Alaska; Figure 2) were used for baseline calculations of percent ice-free surface area per reach and to categorize final spawning locations.

Several preprocessing steps were necessary to convert the SAR images from their original data format to a geocoded product amenable to processing and interpretation. The level 1 data acquired from ASF was processed in Mapready (ASF 2009) to convert it from CEOS format to a GeoTIFF format. This preprocessing step allowed for multi-temporal images to be stacked together in a geographic information system (GIS) for analysis. Ice-free areas were hand-digitized using ArcGIS for all years for which SAR images were available (Figure 3). Once digitizing was complete, layers for the different years were stacked and analyzed for assessing persistence in the occurrence and extent of these areas from year to year. A reach with a persistent ice-free area for each image analyzed was given a value of (1); otherwize, the reach was classified as nonpersistent and given a value of (0). Persistent ice-free areas did not always have the same extent because cold severity affects the degree of ice cover; however, the centroid and overall shape of persistent ice-free areas remained consistent (Figure 4), whereas nonpersistent areas had no overlap from year to year (Figure 3).

Ice-free water classification results for AVNIR-2 imagery give an overall accuracy of 86.2% (Table 3). Unique areas of long-term persistence were identified from the time-series analysis using SAR imagery.

Braiding index and sinuosity.—The braiding index (B) was calculated by the sum of the mid-channel lengths (L_{ctot}) of all the segments of primary channels in a reach and the mid-channel

Downloaded by [University of Missouri Columbia] at 11:54 31 August 2012

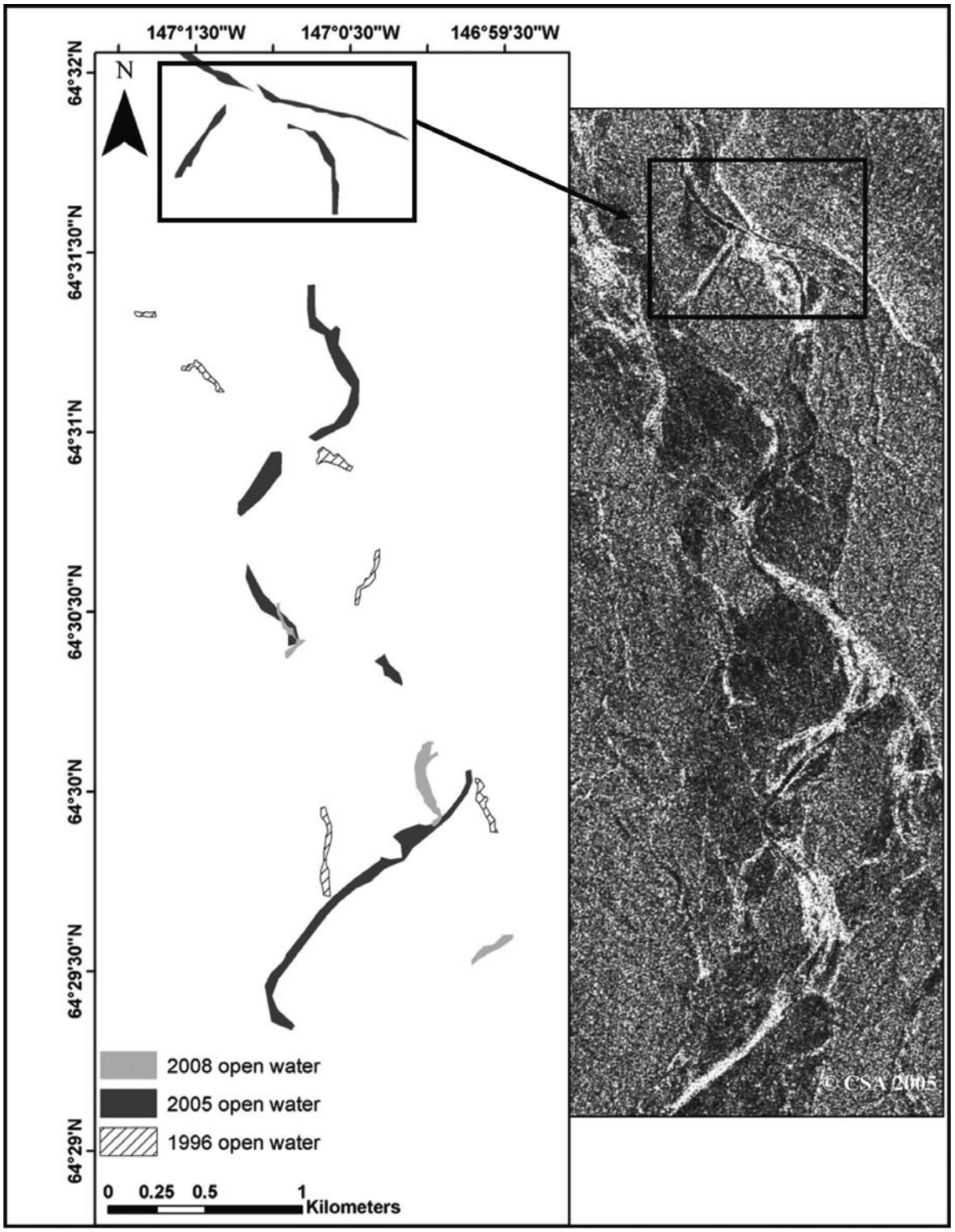

FIGURE 3. Ice-free (open water) areas in the main-stem Tanana River digitized and layered to show a dominant pattern. The location of upwelling areas change with the relocation of the main channel and braiding pattern through time (1996–2008). The arrow is indicating the zone digitized from the 2005 SAR imagery.

Downloaded by [University of Missouri Columbia] at 11:54 31 August 2012

Downloaded by [University of Missouri Columbia] at 11:54 31 August 2012

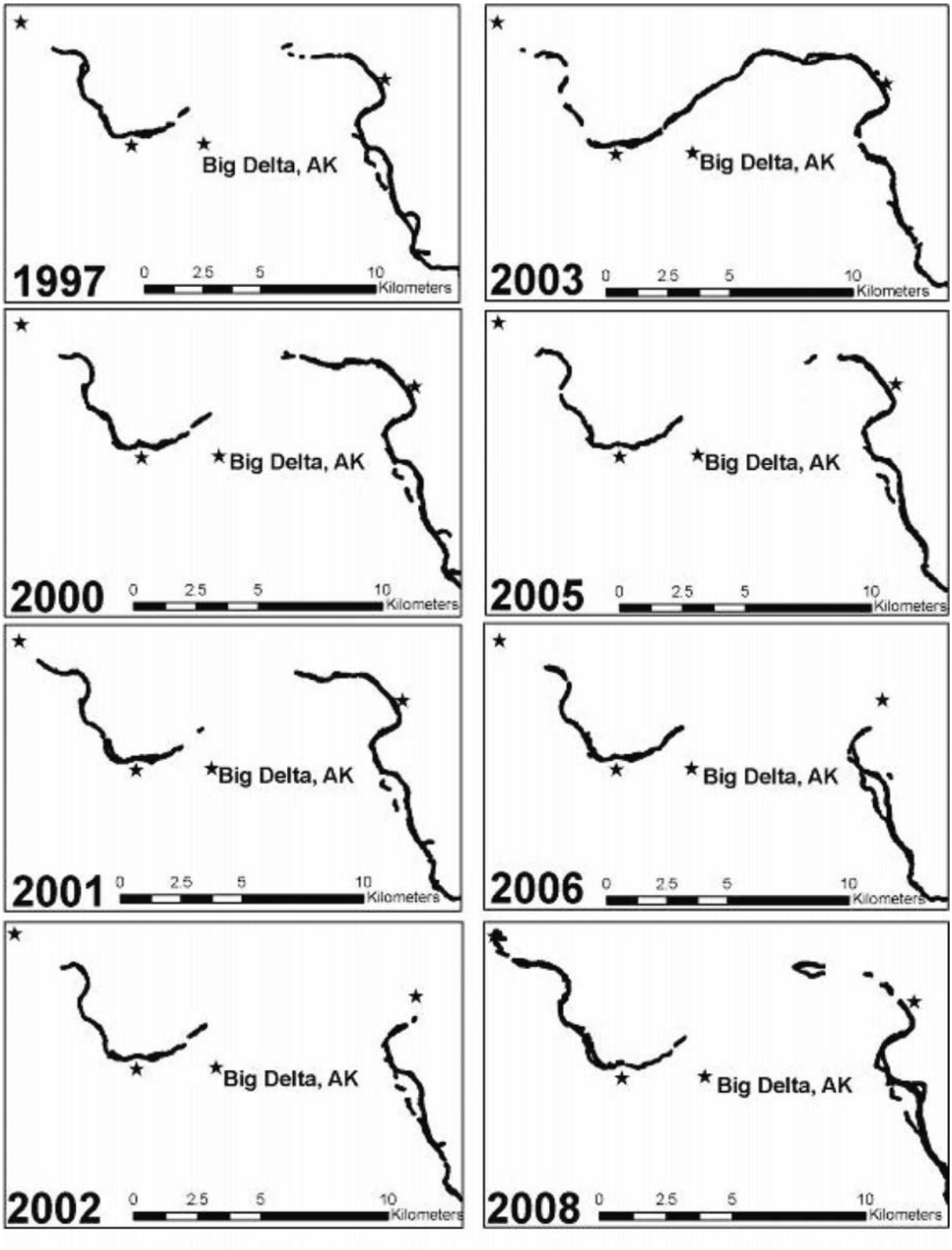

FIGURE 4. Mapped Tanana River ice-free water for each year examined near Big Delta, Alaska. The stars represent fixed locations for each year for location reference. This shows variability in each year for extent of ice-free water and shows two distinct areas that remain open each year studied.

TABLE 3. Accuracy assessment for ice-free (IF) and frozen (FR) classifications of AVNIR-2 imagery.

Reference (ground) data				
Classified data	IF	FR	Total	User's accuracy (%)
IF	5	1	6	83.3
FR	3	20	23	87.0
Total pixels	8	21	29	
Producer's accuracy (%)	62.5	95.2		86.2

length (L_{cmax}) of the widest channel through the reach (Friend and Sinha 1993): $B = L_{ctot}/L_{cmax}$.

Sinuosity (P) was calculated by L_{cmax} and the overall length of the channel (L_R), measured along a straight line (Friend and Sinha 1993): $P = L_{cmax}/L_R$. Ice-free water surface area (km^2) was calculated from AVNIR-2 images from March 2009 by manually digitizing the extents of the water body in ArcGIS (ESRI 2007).

Thermal information.—The optical and SAR imagery provided information to delineate ice-free bodies but did not provide remotely sensed information on water temperatures. Therefore, to address the likely mechanism for that ice-free or the extent of groundwater influence, temperature data loggers were used to characterize water temperatures within areas of ice-free and frozen water. Surface water temperature measurements were collected using HOBO Pro (version 2) water temperature data loggers (Onset 2008) that were deployed in October and November 2008 and continually collected data until retrieval in April 2009. Loggers were placed in eight ice-free locations and 15 frozen locations prior to river freeze-up. These locations were chosen based on visual ice mapping during November–December 2007. Two data loggers were deployed in each ice-free area, one at the upstream end and one at the downstream end. One logger was deployed at each of the frozen water locations.

To obtain quantitative estimates on the water temperatures and gain further insight into the characteristics of areas of groundwater influence, we used Forward-Looking Infrared Radiometer (FLIR) images. In November 2009, FLIR images were collected to describe temperature patterns for selected ice-free areas. The FLIR sensor acquires surface temperature values in a single 7.5–13-μm broadband spectral range. A ThermoVision A320G (FLIR 2009) sensor with a 24° lens was used to capture images at a rate of 30 images/s. Flying at an altitude of 1,300 m provided thermal images with a spatial resolution of 1.7 m. Flying height, ambient temperature, and atmospheric humidity at the time of flight were entered into the FLIR software for automated corrections of the recorded thermal data. The FLIR software uses an inversion of Planck's function to convert spectral radiance to radiant temperature values. We used a uniform emissivity value of 0.90 during image collection. Most natural substances have emissivity values of 0.80–0.97 (Lillesand et al. 2008), and taking a uniform emissivity did not influence the spatial thermal patterns we obtained. The FLIR images collected for specific ice-free sites were loaded into FLIR-builder software that automatically stitched images together. The images were then geo-referenced via ERDAS Imagine software (Leica Geosystems 2008) using the ALOS AVNIR-2 image from March 2009 as the base image for spatial reference.

Habitat modeling and characterization.—We determined final spawning locations from female fall chum salmon through having at least three telemetry points within a single reach within 1 month of each other. This timeframe was chosen to account for time spent by the female searching for a nest site, digging a redd, spawning, and territorial defense. Tagged individuals that traveled through the study area and showed no site fidelity were not included in analysis. The ALOS -AVNIR-2 images acquired in March 2009 were combined with telemetry data to determine final spawning location.

Using negative binomial regression, we constructed a model of habitat use at the reach scale. The negative binomial is a discrete probability distribution that is used for animal count data and considers zero's, inherent in ecological count data (Power and Moser 1999; Pradhan and Leung 2006; Lewin et al. 2010). The SAS statistical package (SAS 2009) was used for all analyses. The dependent variable was total number of spawning salmon per study reach, determined using methods described above. The independent variables were: braiding, sinuosity, ice-free water surface area (determined from 2009 AVNIR-2 images), and persistent ice-free water (determined from SAR images).

We used the information-theoretic approach, and model selection was based on Akaike's information criterion (AIC; Burnham and Anderson 2002). All variables used to create the model of habitat use were tested for covariance by using Pearson's product-moment correlation coefficient (variables excluded from the same model if $R > 0.60$). Persistent ice-free water (hereafter, persistence) covaried significantly with both braiding and ice-free-water surface area ($R = 0.72$), preventing a test of a global model; we instead tested alternative candidate models. Candidate models included sinuosity, braiding, and ice-free-water surface area; braiding and ice-free-water surface area; persistence; and persistence and sinuosity. Without overwhelming evidence for a single best model, we performed model-averaging using Akaike weights (following Burnham and Anderson 2002).

RESULTS

Chum salmon spawned in reaches that not only contained the greatest areas of ice-free water, but also ice-free water that was persistent over the years monitored. Without overwhelming evidence for a single candidate model of the final spawning reach for fall chum salmon (Table 4), we developed an averaged

Downloaded by [University of Missouri Columbia] at 11:54 31 August 2012

TABLE 4. Candidate models of final spawning location for fall chum salmon with intercept and 95% confidence interval in parentheses, R^2, and corrected Akaike information criterion (AIC_c) values calculated from a negative binomial regression analyses. Also shown is the AIC_c difference (Δ) between candidate models used to calculate weights for model averaging. Due to covariance between ice-free persistence and ice-free area, we were unable to construct a global model.

	Variable						
Model	*P* (sinuosity)	*B* (braiding)	Ice-free area	Persistence	R^2	AIC_c	Δ
P, Persistence	4.62 (1.14, 8.10)			−1.51 (−2.17, −0.85)	0.60	68.16	0.00
Persistence				−1.08 (−1.76, −0.42)	0.51	69.52	1.36
B, Ice-free area		0.13 (−0.51, 0.77)	1.62 (0.019, 3.22)		0.33	76.45	8.29
P, B, Ice-free area	1.36,(−2.55, 5.27)	0.06 (−0.59, 0.72)	1.66 (0.021, 3.31)		0.34	78.36	10.20

Downloaded by [University of Missouri Columbia] at 11:54 31 August 2012

model of the most plausible models for predicting number of spawning fall chum salmon. It included sinuosity (parameter estimate = 3.06, 95% CI = 1.14–8.10) and persistence (parameter estimate = 1.36, 95% CI = 0.85–2.17). This averaged model had sizably greater correspondence with spawning counts than the most plausible model that included ice-free-water area ($R = 0.57$ versus $R = 0.33$).

Temperature data loggers were retrieved from 14 of 23 locations in April 2009 (Figure 1). Loggers were retrieved from six locations thought to be frozen based on visual aerial surveys conducted in 2007; however, upon retrieval, locations 1, 2, and 12 were ice-free, and sites 3, 4, and 6 had dried and were completely free of ice (Appendix). The most consistent temperatures through the winter season (adequate for egg incubation) were in location 14, a persistent ice-free site (mean = 4.78°C, range = 3.99–5.8°C). Inconclusive results due to logger loss and drying led us to investigate the thermal characteristics of ice-free locations from the FLIR images.

These images were collected from persistent ice-free areas (spanning 1996–2008) to obtain spatially continuous thermal characteristics on a larger, more continuous scale. These images illustrated the thermal heterogeneity of upwelling water areas and the extent of groundwater thermal influence on surface waters. For corroboration, we compared surface temperature loggers from site 14 with FLIR imagery, and data were in agreement. One image from a spawning habitat site near Rika's Roadhouse displayed warm upwelling water (4.5–6.0°C) entering the system, contrasting with much cooler surface water (1.0°C; Figure 5). A second ice-free area near Bluff Cabin Slough also showed warmer groundwater entering the system. This site contains extensive thermal spatial heterogeneity with strong input of warmer water, presumably from groundwater influx (Figure 6). Two surface water temperature data loggers were retrieved from location 9, which was about 600 m upstream from FLIR image acquisition in the third persistent upwelling site. Both data loggers showed highly variable temperatures, means remaining just above 0.0°C, which suggests limited influence of groundwater in this location.

DISCUSSION

Our observations suggest that spawning chum salmon exhibit strong association with reaches characterized by an increased availability of liquid water in late winter, and the most likely models included information on the spatial and temporal persistence of these habitats, likely driven by groundwater processes. These results suggest that females selected reaches for not only the presence of upwelling water, but also for the stability of groundwater influx. Given that spawning habitat selection is a shorter-term process than groundwater stability over years or decades, this may reflect past reproductive success of previous generations and homing behavior of following generations to reaches with consistent groundwater influences. Alternatively, it could imply that deep groundwater has a different chemical signature that fall chum salmon have evolved to detect and select over areas with groundwater of more shallow and ephemeral origin.

Collection of microhabitat variables for fall chum salmon spawning habitat (e.g., substrate, depth, and velocity) were attempted but unsuccessful due to the dynamic, remote, and logistically challenging nature of a large, glacial river and the season (late fall) that fall chum salmon occupied the habitat. Placement of temperature data loggers based on aerial visual observations resulted in incomplete habitat assessment, where no broad-scale interpretation could be made about fundamental habitat requirements. This led to further examination of temperature patterns within and between upwelling locations using FLIR imagery. Forward-looking infrared images showed extensive thermal heterogeneity within areas influenced by groundwater, but the degree of upwelling influx varied among ice-free locations.

Identifying areas with strong groundwater inputs and complex thermal heterogeneity with FLIR imagery allows for the identification of areas containing a suitable thermal environment for egg incubation and may assist in identification of the first-order control on spawning habitat selection if information on persistent ice-free water is not available. In a concurrent study, the USGS assessed the thermal characteristics of locations in the Tanana River within the area covered by FLIR images.

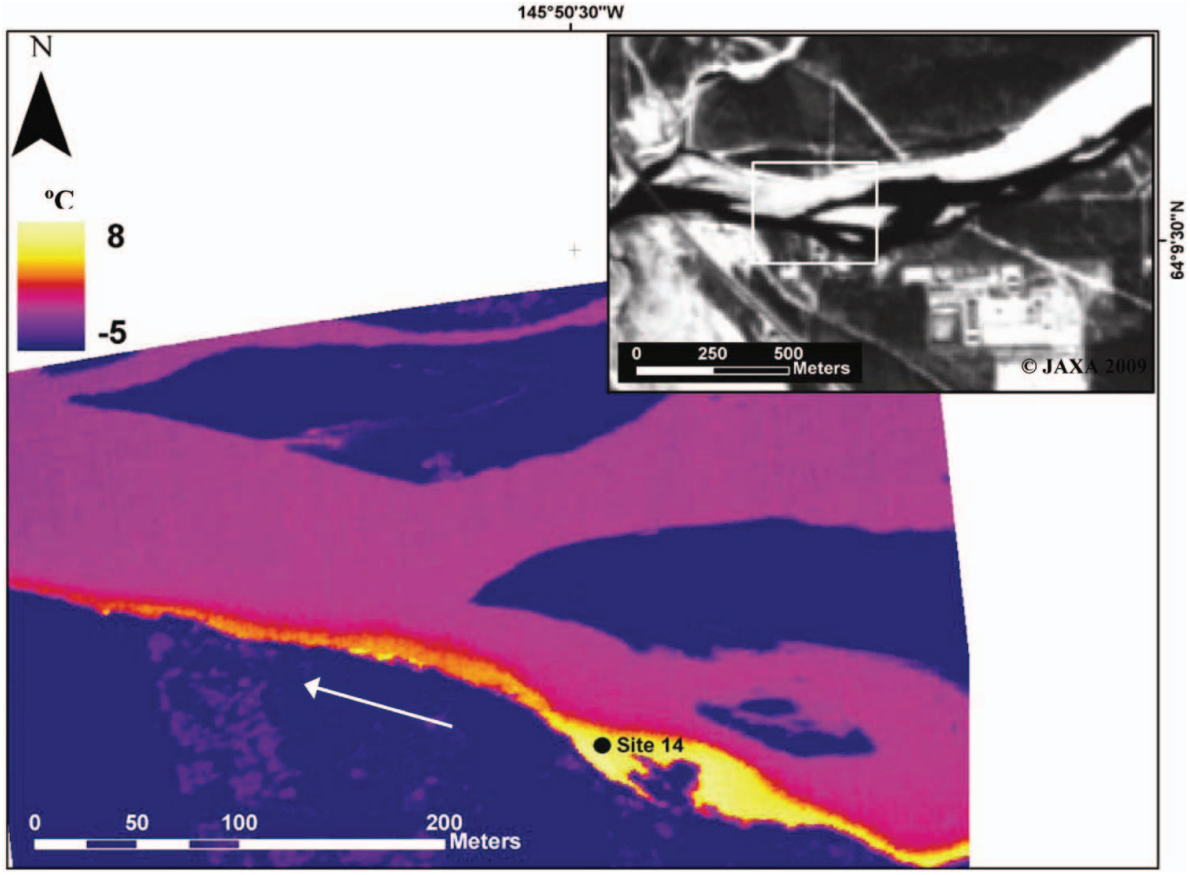

FIGURE 5. Forward-looking infrared (FLIR) image of a fall chum salmon spawning habitat area in the Tanana River near Rika's Roadhouse, showing warm groundwater influx (yellow shaded area) compared with the cooler surface water (pink shaded area). The arrow is flow direction, and the enclosed circle indicates location of surface temperature data logger retrieved from location 14. The inset is showing the AVNIR-2 image used for georeferencing, and in which the white-line box shows the boundaries of the FLIR image. [Figure available in color online.]

Examining the intergravel and surface water temperature characteristics of upwelling habitats, their upwelling habitat locations 9 and 10 had a higher vertical hydraulic gradient and contained stable intergravel temperatures, which provided sufficient accumulated thermal units (an accumulated effect of temperature over time) for complete egg incubation and fry emergence (Figure 6; Table 5; Burril et al. 2010). Surface water temperatures directly in an area of groundwater input were

TABLE 5. List of locations monitored by USGS scientists, reporting vertical hydraulic gradient (VHG), type of logger used, minimum–maximum range, and mean temperatures and accumulated thermal units (ATU) for each site (from Burril and Zimmerman 2010). No temperature data could be retrieved from location 5.

USGS reach location number	VHG (cm)	Data logger	Temperature (°C)			ATU
			Range		Mean	
5	0.2					
9	0.6	Surface	−0.0	5.5	3.1	467
		40 cm 1	1.2	5.8	5.6	842
		40 cm 2	−0.1	5.5	5.2	783
10	1.0	Surface	0.0	4.0	1.0	158
		40 cm 1	5.0	5.4	5.2	779
		40 cm 2	4.7	5.2	5.0	749

Downloaded by [University of Missouri Columbia] at 11:54 31 August 2012

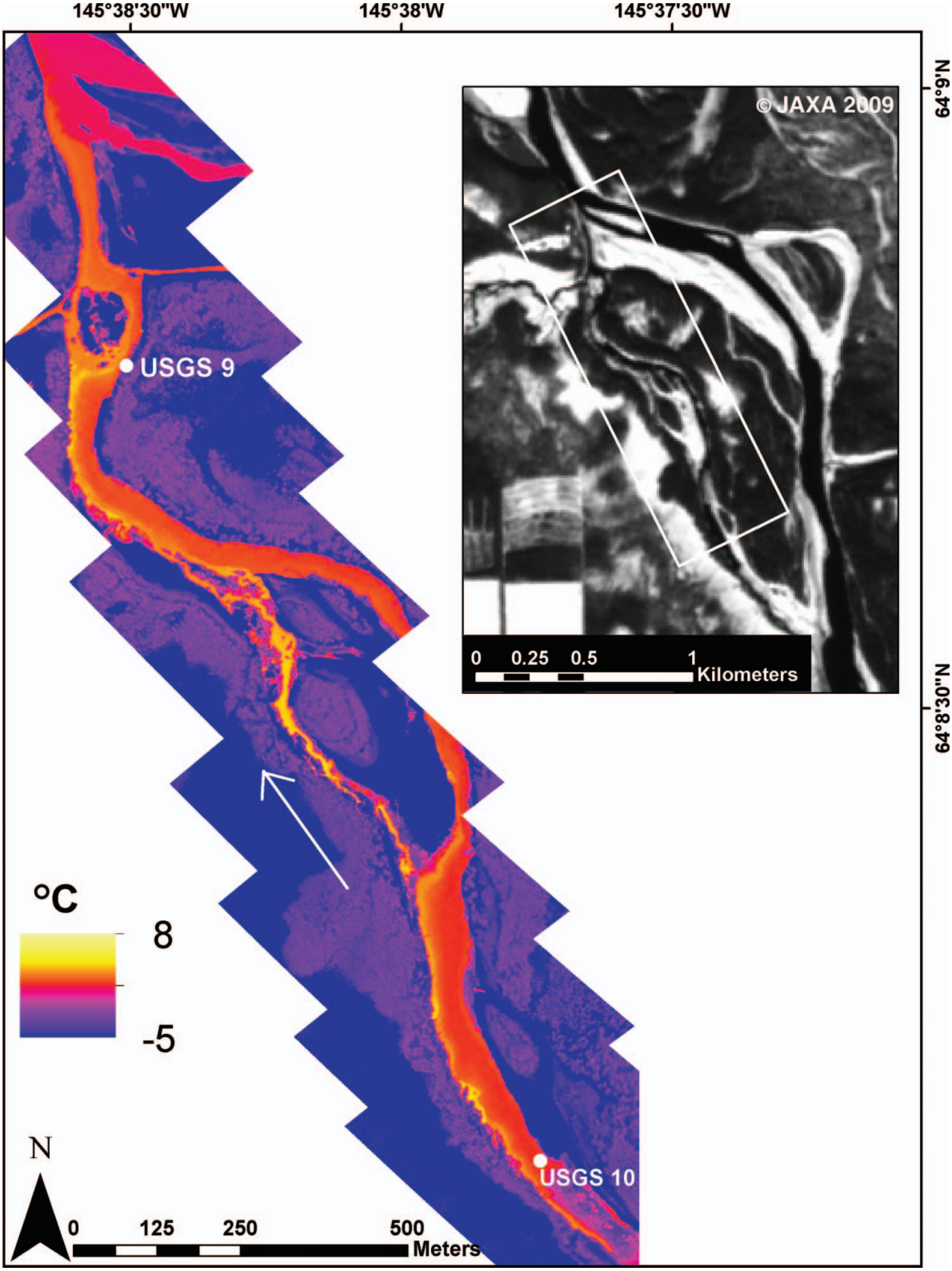

FIGURE 6. Forward-looking infrared (FLIR) image of the Tanana River near Bluff Cabin Slough, displaying spatial thermal heterogeneity of upwelling groundwater influx and the location of Burril's et al. (2010) U.S. Geological Survey sites 9 and 10, which provided corroborating information. The arrow is flow direction The inset is the AVNIR-2 image used for georeferencing within which the white-line box shows the boundaries of the FLIR image. [Figure available in color online.]

Downloaded by [University of Missouri Columbia] at 11:54 31 August 2012

Downloaded by [University of Missouri Columbia] at 11:54 31 August 2012

stable and similar to intergravel temperatures. Surface water temperatures not directly in an area of groundwater influx, but in close proximity, varied significantly, though intergravel temperatures remained stable. These data illustrate the utility of integrating remote sensing and in-stream data collection to identify critical habitat for spawning fall chum salmon and to investigate the role of the abiotic environment in habitat selection. This would only apply to areas of the river with sufficient mixing and turbulence to permit groundwater-influenced waters to thermally mix with surface waters.

It has been argued that traditional habitat assessment methods employed in a stochastic (snapshot) manner only examine small spatial and temporal phenomena and fail to capture important ecological and physical processes important to fish productivity (Geist and Dauble 1998; Baxter and Hauer 2000; Fausch et al. 2002). Applying traditional habitat-assessment methods for small streams to the large, glacially fed Tanana River proved infeasible, necessitating the acquisition of remotely sensed data. Recent advancements in technology have allowed for the use of optical remote sensing of in-stream habitat features important for juvenile salmon at intermediate scales (Carbonneau et al. 2005a; Carbonneau et al. 2005b; Carbonneau et al. 2006; Smikrud and Prakash 2006; Marcus and Fonstad 2008; Smikrud et al. 2008; Woll et al. 2011). However, in the arctic regions, high solar incidence angles due to the high latitude and frequent cloud cover are common problems. The use of SAR imagery circumvented these problems and allowed for the identification of persistent ice-free habitats important in the two most likely models. However, it was also crucial to include optical data with greater spectral contrast (when available for our study location) to verify and substantiate our visual interpretation of SAR imagery.

The strong selection of spatially and temporally persistent ice-free areas identifies the role of both the presence and temporal stability of this critical habitat for this species. Ephemeral ice-free areas in the main-stem Tanana River are probably dominated by hyporheic flow with smaller, less stable groundwater input. The hyporheic zone where surface water and groundwater interact to influence ecological processes in rivers and streams (Boulton et al. 1998) is controlled by geomorphology (Poole et al. 2006) and can have a strong influence on riverine landscapes (Wiens 2002). Geomorphology and complex patterns of hyporheic exchange and upwelling are important for spawning bull trout *Salvelinus confluentus* (Baxter and Hauer 2000) and brook trout *Salvelinus fontinalis* (Curry et al. 1995). Ice-free areas have provided rearing habitat for juvenile Chinook salmon *Oncorhynchus tshawytscha* during winter in British Columbia (Levings and Lauzier 1991). Trout population densities are generally highest in streams with high groundwater discharge (Fausch et al. 1988).

Now that the surface water and groundwater interaction has been identified in critical habitat areas, the next step is to conduct in-stream analysis to identify water chemistry characteristics within and between upwelling areas. It would be illustrative to connect the characteristics of groundwater directly to reproductive success via direct investigation of chum salmon redds. Generally, groundwater may be low in dissolved oxygen and perhaps detrimental to salmon embryo survival (Sowden and Power 1985; Malcolm et al. 2004). However, complex hydrological patterns with strong upwelling and localized downwelling can lead to higher oxygen concentrations suitable for spawning salmonids (Baxter and Hauer 2000). Use of FLIR imagery to identify areas of groundwater influx with complex patterns will aid in targeted in-stream analysis to identify localized downwelling. Additional water chemistry analyses of complex surface water and groundwater mixing environments, identified from FLIR imagery, could potentially identify important chemical cues that spawning fall chum salmon are using to home to spawning grounds. These types of studies can help biologists hone in on localized and important habitats, while elucidating reach and site-scale variables for salmon and better determine physical processes creating and maintaining these habitats.

Although the highest densities of fish were in persistent ice-free habitats, many individuals spawned in areas that eventually froze over. This does not necessarily imply that these individuals were ultimately unsuccessful in their reproductive effort or that they did not select areas where upwelling was taking place. The presence of ice-free water in winter merely indicated sufficient upwelling influence to prevent surface freezing. Alternatively, a lack of ice cover only indicated, but did not directly measure, the presence of groundwater; however, we are confident that any unfrozen water prior to spring thaw in March is the result of groundwater influence, given the severity and length of the sub-zero temperatures of the Alaska winter. However, the fact remains that we did not have the means to observe upwelling phenomena directly at a large spatial extent.

With these caveats in place, we present strong evidence that spatially and temporally persistent upwelling areas with complex surface water and groundwater interactions provide core habitats essential for fall chum salmon population productivity and persistence. Reaches with groundwater influence but lower stability and influence may alternatively offer reproductive habitat for straying fish or fish that are competitively excluded from the core areas. In unstable zones, the continued presence of spawning chum salmon in consecutive years may be due to the influx of individuals into potential sinks from core habitats (Dunning et al. 1992). Further analysis of groundwater input in nonpersistent upwelling areas is necessary to better explain fall chum salmon spatial distributions and determine whether they are truly sink habitats. A common practice in habitat conservation is to prioritize protection of core productive habitats. Typically, these habitats have the largest densities of individuals, are resistant to declines, and offer a source for future emigration to unoccupied habitats (Isaak and Thurow 2006). Although these core areas are clearly important, this conservation strategy can have long-term consequences by constraining populations in the event that core habitats are lost

Downloaded by [University of Missouri Columbia] at 11:54 31 August 2012

and no peripheral populations are available to recolonize core areas.

Hubbs and Trautman (1935) drew attention to the need for winter investigations of freshwater fish populations. Although winter studies have increased since that call, they remain challenging and underrepresented in the ecological literature. Winter research is not only particularly challenging, but particularly important in high-latitude regions like Alaska, where winter conditions are severe and small areas of the landscape can have disproportionate importance for the persistence and productivity of fish populations (Reynolds 1997). Transferring the methods used in this study across high latitude river systems has the potential to alleviate logistical challenges associated with working outdoors in the arctic environment.

According to current climate change predictions, arctic freshwater systems will warm more rapidly than the global average, particularly during winter (Prowse et al. 2006). A warming climate is likely to create hydrologic shifts in freshwater river systems, changing seasonal flow, ice cover, and the severity of freeze-up and break-up (Prowse et al. 2006). Studies using winter stream flow as a proxy for groundwater inputs in the Yukon River basin are indicating shifts in surface water and groundwater interactions, with an increase in groundwater contributions to overall stream flow due to permafrost thawing, increasing dissolved inorganic carbon and nitrogen (Striegl et al. 2007; Walvoord and Striegl 2007). It is essential to understand the current chemistry, particularly oxygen levels, of upwelling areas important for salmon spawning if warming events cause a change in groundwater processes and, therefore, the chemical environment of the river. Our study demonstrates that combining remote sensing and in-stream evaluations will allow researchers to create baseline information for monitoring salmon spawning habitat in areas that may be most vulnerable to climate change but have received little attention due to inaccessibility and inadequate survey methods.

ACKNOWLEDGMENTS

This research was funded through the Arctic Yukon Kuskokwim Sustainable Salmon Initiative, the Commercial Fisheries Division of the Alaska Department of Fish and Game, and the Tanana Chiefs Conference. The latter two operated the fish wheel that captured the study fish and tracked fish via radiotelemetry, and they generously provided those data for our study. We would like to thank R. Driscoll, A. Merriman, B. Baker, P. Drobny, C. Zimmerman, S. Burril, and V. von Biela for help with field work; R. Gens for help with SAR data processing and interpretation; W. Witte and W. Putman for assistance with GIS; and G. Wirth for computational and field work support. We acknowledge the Alaska Satellite Facility for providing the SAR and ALOS data at no cost for this research. The ALOS data were processed and provided by the Americas ALOS Data Node. Sincere thanks to Chena River Aviation, Quicksilver Air, Inc., Teraterpret, Ken Air, and Webster's Flying Service for providing safe flights for data acquisition. The use of trade or product names does not imply endorsement by the U.S. Government.

REFERENCES

ASF (Alaska Satellite Facility). 2009. MapReady, version 2.1. ASF, Fairbanks.

ATS (Advanced Telemetry Systems). 2008. World's most reliable wildlife transmitters and tracking systems. ATS, Isanti, Minnesota. Available: www.atstrack.com./ (June 2010).

Barton, L. H. 1992. Tanana River, Alaska, fall chum salmon radio telemetry study. Alaska Department of Fish and Game, Division of Commercial Fisheries, Fishery Research Bulletin 92-01, Juneau.

Baxter, C. V., and F. R. Hauer. 2000. Geomorphology, hyporheic exchange, and selection of spawning habitat by bull trout (*Salvelinus confluentus*). Canadian Journal of Fisheries and Aquatic Sciences 57:1470–1481.

Borba, B. M., D. J. Bergstrom, and F. J. Bue. 2009. Yukon River fall chum salmon stock status and fall season salmon fisheries, 2009: a report to the Alaska board of fisheries. Alaska Department of Fish and Game, Division of Commercial Fisheries, Special Publication 09-24, Anchorage.

Boulton, A. J., S. Findlay, P. Marmonier, E. H. Stanley, and H. M. Valett. 1998. The functional significance of the hyporheic zone in streams and rivers. Annual Review of Ecology and Systematics 29:59–81.

Bue, F. J., B. M. Borba, and D. J. Bergstrom. 2004. Yukon River fall chum salmon stock status and action plan. Alaska Department of Fish and Game, Division of Commercial Fisheries, Regional Information Report 3A04-05, Anchorage.

Burnham, K. P., and D. R. Anderson. 2002. Model selection and multimodel inference: a practical information-theoretic approach, 2nd edition. Springer-Verlag, New York.

Burril, S. E., C. E. Zimmerman, and J. E. Finn. 2010. Characteristics of fall chum salmon spawning habitat on a mainstem river in interior Alaska. U.S. Geological Survey, Open-File Report 2010-1164, Reston, Virginia.

Carbonneau, P. E., N. Bergeron, and S. N. Lane. 2005a. Automated grain size measurements from airborne remote sensing for long profile measurements of fluvial grain sizes. Water Resources Research 41:article W11426. DOI: 10.1029/2005WR003994.

Carbonneau, P. E., N. E. Bergeron, and S. N. Lane. 2005b. Texture-based image segmentation applied to the quantification of superficial sand in salmonid river gravels. Earth Surface Processes and Landforms 30:121–127.

Carbonneau, P. E., S. N. Lane, and N. Bergeron. 2006. Feature based image processing methods applied to bathymetric measurements from airborne remote sensing in fluvial environments. Earth Surface Processes and Landforms 31:1413–1423.

Cumming, I. G., and F. H. Wong. 2005. Digital processing of synthetic aperture radar data: algorithms and implementation. Artech House, Norwood, Massachusetts.

Curry, R. A., D. L. G. Noakes, and G. E. Morgan. 1995. Groundwater and the incubation and emergence of brook trout (*Salvelinus fontinalis*). Canadian Journal of Fisheries and Aquatic Sciences 52:1741–1749.

Dunning, J. B., B. J. Danielson, and H. R. Pulliam. 1992. Ecological processes that affect populations in complex landscapes. Oikos 65:169–175.

ESRI (Environmental Systems Research Institute). 2007. ARC/INFO GIS, version 9.2. ESRI, Redlands, California.

Fausch, K. D., C. L. Hawkes, and M. G. Parsons. 1988. Models that predict standing crop of stream fish from habitat variables: 1950–85. U.S. Department of Agriculture, Forest Service, Pacific Northwest Research Station, General Technical Report PNW-GTR-213, Portland, Oregon.

Fausch, K. D., C. E. Torgersen, C. V. Baxter, and H. W. Li. 2002. Landscapes to riverscapes: bridging the gap between research and conservation of stream fishes. BioScience 52:483–498.

FLIR (Forward-Looking Infrared Radiometer). 2009. The world leader in thermal imaging. FLIR Systems, Boston, Massachusetts. Available: http://www.flir.com./ (June 2010).

Friend, P. F., and R. Sinha. 1993. Braiding and meandering parameters. Pages 105–111 *in* J. L. Best and C. S. Bristow, editors. Braided rivers. Geological Society, Special Publication 75, London.

Fung, A. K., and F. T. Ulaby. 1983. Matter-energy interaction in the microwave region. Pages 115–161 *in* D. S. Simonett and F. T. Ulaby, editors. Manual of remote sensing. American Society of Photogrammetry, Falls Church, Virginia.

Geist, D. R., and D. D. Dauble. 1998. Redd site selection and spawning habitat use by fall Chinook salmon: the importance of geomorphic features in large rivers. Environmental Management 22:655–669.

Geist, D. R., T. P. Hanrahan, E. V. Arntzen, G. A. McMichael, C. J. Murray, and Y. J. Chien. 2002. Physicochemical characteristics of the hyporheic zone affect redd site selection by chum salmon and fall Chinook salmon in the Columbia River. North American Journal of Fisheries Management 22:1077–1085.

Gens, R. 2009. Spectral information content of remote sensing imagery. Pages 177–201 *in* D. Li, J. Shan, and J. Gong, editors. Geospatial technology for earth observation. Springer, New York.

Hausle, D. A., and D. W. Coble. 1976. Influence of sand in redds on survival and emergence of brook trout (*Salvelinus fontinalis*). Transactions of the American Fisheries Society 105:57–63.

Hubbs, C. L., and M. B. Trautman. 1935. The need for investigating fish conditions in winter. Transactions of the American Fisheries Society 65:51–56.

Isaak, D. J., and R. F. Thurow. 2006. Network-scale spatial and temporal variation in Chinook salmon (*Oncorhynchus tshawytscha*) redd distributions: patterns inferred from spatially continuous replicate surveys. Canadian Journal of Fisheries and Aquatic Sciences 63:285–296.

Lapointe, M. F., N. E. Bergeron, F. Bérubé, M. A. Pouliot, and P. Johnston. 2004. Interactive effects of substrate sand and silt contents, redd-scale hydraulic gradients, and interstitial velocities on egg-to-emergence survival of Atlantic salmon (*Salmo salar*). Canadian Journal of Fisheries and Aquatic Sciences 61:2271–2277.

Leica Geosystems. 2008. ERDAS imagine, version 9.1. Leica Geosystems, Atlanta, Georgia.

Levasseur, M., N. E. Bergeron, M. F. Lapointe, and F. Bérubé. 2006. Effects of silt and very fine sand dynamics in Atlantic salmon (*Salmo salar*) redds on embryo hatching success. Canadian Journal of Fisheries and Aquatic Sciences 63:1450–1459.

Levings, C. D., and R. B. Lauzier. 1991. Extensive use of the Fraser River basin as winter habitat by juvenile Chinook salmon (*Oncorhynchus tshawytscha*). Canadian Journal of Zoology 69:1759–1767.

Lewin, W. C., J. Freyhof, V. Huckstorf, T. Mehner, and C. Wolter. 2010. When no catches matter: coping with zeros in environmental assessments. Ecological Indicators 10:572–583.

Lillesand, T. M., R. W. Kiefer, and J. W. Chipman. 2008. Remote sensing and image interpretation, 6th edition. Wiley, New York.

Malcolm, I. A., C. Soulsby, A. F. Youngson, D. M. Hannah, I. S. McLaren, and A. Thorne. 2004. Hydrological influences on hyporheic water quality: implications for salmon egg survival. Hydrological Processes 18:1543–1560.

Marcus, W. A., and M. A. Fonstad. 2008. Optical remote mapping of rivers at sub-meter resolutions and watershed extents. Earth Surface Processes and Landforms 33:4–24.

Milner, A. M., J. G. Irons III, and M. W. Oswood. 1995. The Alaskan landscape: an introduction for limnologists. Pages 2–44 *in* A. M. Milner and M. W. Oswood, editors. Freshwaters of Alaska: ecological syntheses. Springer-Verlag, New York.

Onset. 2008. Data loggers from the world leader. Onset, Bourne, Massachusetts. Available: www.onsetcomp.com./ (June 2010).

Osterkamp, T. E. 1975. Observations of Tanana River ice. Pages 201–208 *in* G. E. Frankenstein, editor. Proceedings third international symposium on ice problems. International Association of Hydraulic Research, Madrid.

Pietroniro, A., J. Töyrä, R. Leconte, and G. Kite. 2005. Remote sensing of surface water and soil moisture. Pages 119–142 *in* C. R. Duguay and A. Pietroniro, editors. Remote sensing in northern hydrology: measuring environmental change. American Geophysical Union, Washington, D.C.

Poole, G. C., J. A. Stanford, S. W. Running, and C. A. Frissell. 2006. Multiscale geomorphic drivers of groundwater flow paths: subsurface hydrologic dynamics and hyporheic habitat diversity. Journal of the North American Benthological Society 25:288–303.

Power, J. H., and E. B. Moser. 1999. Linear model analysis of net catch data using the negative binomial distribution. Canadian Journal of Fisheries and Aquatic Sciences 56:191–200.

Pradhan, N. C., and P. S. Leung. 2006. A Poisson and negative binomial regression model of sea turtle interactions in Hawaii's longline fishery. Fisheries Research 78:309–322.

Prowse, T. D., F. J. Wrona, J. D. Reist, J. J. Gibson, J. E. Hobbie, L. M. J. Lévesque, and W. F. Vincent. 2006. Climate change effects on hydroecology of Arctic freshwater ecosystems. Ambio 35:347–358.

Quinn, T. P. 2005. The behavior and ecology of Pacific salmon and trout. American Fisheries Society, Bethesda, Maryland.

Reynolds, J. B. 1997. Ecology of overwintering fishes in Alaskan freshwaters. Pages 281–302 *in* A. M. Milner and M. W. Oswood, editors. Freshwaters of Alaska: ecological syntheses. Springer-Verlag, New York.

Salo, E. O. 1991. Life history of chum salmon (*Oncorhynchus keta*). Pages 231–309 *in* C. Groot and L. Margolis, editors. Pacific salmon life histories. University of British Columbia Press, Vancouver.

SAS (Statistical Analysis Systems). 2009. SAS 9.1.3: help and documentation. SAS Institute, Cary, North Carolina.

Seeb, L. W., and P. A. Crane. 1999. High genetic heterogeneity in chum salmon in western Alaska, the contact zone between northern and southern lineages. Transactions of the American Fisheries Society 128:58–87.

Simonett, D. S., and R. E. Davis. 1983. Image analysis–active microwave. Pages 1125–1179 *in* D. S. Simonett and F. T. Ulaby, editors. Manual of remote sensing. American Society of Photogrammetry, Falls Church, Virginia.

Smikrud, K. M., and A. Prakash. 2006. Monitoring large woody debris dynamics in the Unuk River, Alaska, using digital aerial photography. GIScience and Remote Sensing 43:142–154.

Smikrud, K. M., A. Prakash, and J. V. Nichols. 2008. Decision-based fusion for improved fluvial landscape classification using digital aerial photographs and forward looking infrared images. Photogrammetric Engineering and Remote Sensing 74:903–911.

Sowden, T. K., and G. Power. 1985. Prediction of rainbow trout embryo survival in relation to groundwater seepage and particle size of spawning substrates. Transactions of the American Fisheries Society 114: 804–812.

Stearns, S. C. 1977. The evolution of life history traits: a critique of the theory and a review of the data. Annual Review of Ecology and Systematics 8: 145–171.

Striegl, R. G., M. M. Dornblaser, G. R. Aiken, K. P. Wickland, and P. A. Raymond. 2007. Carbon export and cycling by the Yukon, Tanana, and Porcupine rivers, Alaska, 2001–2005. Water Resources Research 43:article W02411. DOI: 10.1029/2006WR005201.

Thomson, J. R., M. P. Taylor, K. A. Fryirs, and G. J. Brierley. 2001. A geomorphological framework for river characterization and habitat assessment. Aquatic Conservation: Marine and Freshwater Ecosystems 11: 373–389.

Walvoord, M. A., and R. G. Striegl. 2007. Increased groundwater to stream discharge from permafrost thawing in the Yukon River basin: potential impacts on lateral export of carbon and nitrogen. Geophysical Research Letters 34:article L12402. DOI: 10.1029/2007GL030216.

Wiens, J. A. 2002. Riverine landscapes: taking landscape ecology into the water. Freshwater Biology 47:501–515.

Woll, C., A. Prakash, and T. Sutton. 2011. A case-study of in-stream juvenile salmon habitat classification using decision-based fusion of multispectral aerial images. Applied Remote Sensing Journal 2:37–46.

Downloaded by [University of Missouri Columbia] at 11:54 31 August 2012

APPENDIX: DATA LOGGER INFORMATION

TABLE A.1. Basic data for surface temperature data loggers retrieved from the Tanana River in April 2009. Location identification numbers 5, 7, 9, and 13 contained two loggers.

					Temperature (°C)		
Location number	Latitude	Longitude	Start date	Stop date	Range		Mean
1	64.787	−147.761	Oct 25, 2008	Apr 8, 2009	0.02	2.50	0.78
2	64.769	−147.563	Nov 3, 2008	Apr 6, 2009	1.13	6.36	2.92
3	64.747	−147.438	Nov 3, 2008	Apr 6, 2009	−10.44	2.77	0.84
4	64.686	−147.311	Oct 31, 2008	Apr 8, 2009	−4.90	0.85	−1.20
5	64.677	−147.283	Nov 25, 2008	Apr 6, 2009	−12.31	4.95	−0.22
5	64.677	−147.283	Nov 25, 2008	Apr 6, 2009	−9.44	1.97	0.02
6	64.629	−147.228	Nov 3, 2008	Apr 6, 2009	−8.36	6.97	0.08
7	64.548	−147.066	Nov 25, 2008	Apr 6, 2009	−5.67	2.29	0.82
7	64.548	−147.067	Nov 25, 2008	Apr 6, 2009	−9.37	1.72	0.08
8	64.441	−147.031	Nov 25, 2008	Apr 6, 2009	−4.38	3.14	0.20
9	64.309	−146.828	Nov 25, 2008	Apr 6, 2009	−0.06	3.04	0.79
9	64.309	−146.829	Nov 25, 2008	Apr 6, 2009	−0.12	3.62	0.58
10	64.283	−146.412	Nov 25, 2008	Apr 7, 2009	0.02	0.36	0.05
11	64.249	−146.263	Nov 25, 2008	Apr 9, 2009	0.08	3.85	1.18
12	64.176	−145.888	Nov 3, 2008	Apr 7, 2009	−0.06	3.78	2.24
13	64.156	−145.875	Nov 25, 2008	Apr 7, 2009	−3.72	1.48	0.17
13	64.156	−145.874	Nov 25, 2008	Apr 7, 2009	−9.51	1.51	−1.40
14	64.157	−145.841	Dec 5, 2008	Apr 4, 2009	3.99	5.80	4.78

Downloaded by [University of Missouri Columbia] at 11:54 31 August 2012